GENOME EDITING OF *TAS4, MIR828* AND TARGETS *MYBA6/A7*: A CRITICAL TEST OF *XYLELLA FASTIDIOSA* INFECTION AND SPREADING MECHANISMS IN PIERCE'S DISEASE

Principal Investigator:
Chris Rock
Texas Tech University
Dept of Biological Sciences
Lubbock, TX 79409-3131
chris.rock@ttu.edu

Research Associate:
Sunitha Sukumaran
Texas Tech University
Dept of Biological Sciences
Lubbock, TX 79409-3131
sunitha.sukumaran@ttu.edu

Graduate Research Assistant:
Md. Fakhrul Azad
Texas Tech University
Dept of Biological Sciences
Lubbock, TX 79409-3131
fakhrul.azad@ttu.edu

Cooperator:
David Tricoli
University of California, Davis
Plant Transformation Facility
Davis, CA 95616
dmtricoli@ucdavis.edu

Cooperator:
Leonardo De La Fuente
Auburn University
Dept Entomology& Plant Pathology
Auburn, AL 36849
lzd0005@auburn.edu

FINAL REPORT: The results reported are for work conducted from July 1, 2015- Dec 31, 2017. New results from Nov. 1- Dec. 31, 2017 are reported that make this final report different than the progress report published in the 2017 PD Research Symposium Proceedings.

ABSTRACT (LAYPERSON SUMMARY)

The bacterium *Xylella fastidiosa* (XF) is the cause of Pierce's disease (PD) in grapes and is a major threat to fruit, nut, olive, and coffee groves. The most damaging effect of PD other than death of the vine is the reduction of production, and shriveling of fruits. Obvious symptoms in grapevine are characteristic bands/rings of anthocyanin (red pigment) accumulation in distal zones adjacent to necrotic leaf blades. Anthocyanins can reduce insect feeding, and induction in vegetative tissues may serve as antagonists to feeding by Glassy Winged Sharpshooter (GWSS) and to colonization by XF. The etiology of pleiotropic PD symptoms such as 'matchstick petioles' and 'green cane islands' is not understood. In this context it is noted that Grapevine Red Blotch and Leaf Roll-associated viruses cause similar pleiotropic symptoms because their genomes encode small RNA suppressor proteins evolved to disrupt host microRNA (miRNA) biogenesis and/or activity. Prior work by the Cooperator (DLF) showed that XF infection causes a significant decrease in leaf elemental phosphorus (P) content, but the bioavailable form of P (e.g. phosphoproteins, lipids, nucleic acids, subcellular compartmentation, etc.) underlying this phenomenon is unknown. The myriad host responses to XF are hypothesized to be due to deranged host inorganic phosphate (P_i) -regulated miRNA activities (both P_i and miRNAs are diffusible signals in plants). The data generated in two initial years of PD/GWSS support is compelling and supports our testable model of phosphate-regulated miRNAs synergizing with *MIR828*/*TAS4* to regulate anthocyanin levels. Deep sequencing of miRNAs and their targets in XF-infected leaves, petioles, and cane bark is completed. Further analysis new sequence data forthcoming in the next weeks will allow a systematic and comprehensive view of gene activities and their roles in etiology of PD. A CRISPR/Cas9 genome-editing approach has generated transgenic plants to directly test the model by disrupting host *MIR828* or four downstream effector genes for anthocyanin regulation to determine their roles in susceptibility to XF, and whether they function to impact GWSS feeding preferences. We are also testing a corollary of the working hypothesis: whether a durable, affordable, and environmentally sound 'safener/ protectant' analogue of P_i (phosphite; reduced P_i), which alters host and/or microbe phosphate homeostasis, can impact XF growth and host PD etiology. This aspect could result in development of a novel management tool for PD complementary to the primary high-priority genome editing approach to engineer PD resistance. Genome editing is akin to breeding in that it can produce non-"genetically modified organism" (GMO) grapevines and rootstocks after outcrossing the transgene locus. These proof-in-principle experimental results offer a new paradigm for PD management with potential translational benefits for other crops.

INTRODUCTION

Our working model of PD etiology postulates miR828 and evolutionarily-related *Trans-Acting Small-interfering locus4* (*TAS4*) activities silence MYeloBlastosis (MYB) transcription factor targets *VvMYBA6/A7* and other homologous *MYB* expression in response to XF infection, mediated through inorganic phosphate (P_i) and plant stress hormone abscisic acid (ABA) signaling crosstalk. We are testing the XF infection/spread hypothesis directly by "knocking out" the key hypothesized genes using a new genome editing technology- Clustered Regularly Interspaced Short Palindromic Repeats (CRIPSR/Cas9)[1, 2] that the CDFA-PD Board nominated as a feasible, high-priority approach to engineering PD resistance. A direct test of the model in grapevine by genome editing of the positive and negative anthocyanin effector loci is well grounded now, based on our baseline deep sequencing evidence for miR828/*TAS4* roles in PD, and the completion of the regeneration stage for the subject transgenics.

We have taken a complementary "overexpression" approach to the long-term grapevine MYB target gene knockout/editing approach to test the anthocyanins-as-XF-effectors hypothesis. The surrogate tobacco XF infection system developed by the Cooperator (DLF)[3] can quickly assess susceptibility to XF infection of a transgenic tobacco line[4] (Myb237) that over-expresses the Arabidopsis orthologue of VvMYBA6/A7: *PRODUCTION OF ANTHOCYANIN PIGMENT2/MYB90*. We have generated strong data-driven evidence from our mRNA-Seq, sRNA-Seq and degradome datasets from XF- infected grape and tobacco materials, quantitation of leaf and cane xylem sap concentrations of P_i and anthocyanins in PD-infected field materials, and disease severity correlations with molecular phenotypes from greenhouse XF challenge experiments. Results support a refined model that XF is using host small RNAs as a 'trojan horse' that could serve as a paradigm to understand not only P_i (and miRNAs) as diffusible signals for synthesis of host polyphenolic anti-bacterial metabolites in PD etiology, but also the pleiotropic traits of "green islands" and "matchstick petioles," among others. Our results to date for XF differentially regulated miRNAs in tobacco are completely novel, and what emerges is evidence for a deeply conserved autoregulatory loop for MYB/TAS4/MIR828 co-expression and a highly correlated network of miRNA/phased small-interfering RNA-producing- and *TAS* noncoding loci known to function in plant immunity across plant taxa.

We summarize in **Table I** a chronological list of efforts over the duration of the award and conclusions drawn from experiments documented in CDFA-PD progress reports from July 2015- Octotber 2017. These studies have leveraged a systems approach, building on the miRNA candidate leads to discover etiological effectors/reporters of PD and network analyses of gene interactions affecting primary and secondary metabolism. A direct test of the model in grapevine (Objective I) by genome editing of the positive and negative effector loci is grounded now, based on our deep sequencing evidence for miR828/*TAS4* roles in PD and completion of grapevine regeneration of the subject transgenic lines.

Table I. Timeline of the project activities and results since inception July 2015, reported previously

Report Venue	Activity	Experimental Results
2015 CDFA-PD Proceedings^	-methods development for quantitation of anthocyanins -collect field samples from GA and Temecula CA	engineered five binary T-DNA Agrobacterium CRISPR vectors[1]; phytoene desaturase extra target vectors
Mar. 2016 Interim Progress Report*	-Initiate grapevine transformations -Characterize expression of *TAS4* in transgenic tobacco over-expressing AtMYB90 in response to XF infection; correlate with disease symptom severity and XF titre -spectroscopic quantitation of anthocyanins in PD grapevines from GA and CA fields -initiate grapevine and tobacco small RNA libraries	transformation problem noted; solved later by using different Agrobacterium strain. Homozygous tobacco MYB90 over-expression line more susceptible to XF; correlated with *TAS4* induction by RNA blot.

July 2016 Year-end Progress Report*	-repeat grapevine transformations -showed by immunoblot binary T-DNA CRISPR vector effector Cas9 expressed in *N. benthamiana* -transformed tobacco with CRISPR vectors -initiate RNA-seq libraries of grapevine	Small RNA libraries show strong (~5-fold) induction of *TAS4* by XF infection of grapevine and tobacco; induction degree correlates with phenotypic severity of symptoms in tobacco genotypes.
July 2016 one year project renewal	-Added **Objective III**: xylem sap and leaf P_i quantitation; phosphite effects on XF -Co-I De La Fuente opts for Cooperator role	
2016 CDFA-PD Proceedings^	-develop PAGE heteroduplex genotyping assay -repeat tobacco XF challenge experiment -DESeq2 statistical analysis of differential miRNA expression by XF on 2015 CA libraries -complete RNA-Seq libraries and initiate degradome libraries on 2015 CA samples -In vivo nuclear magnetic resonance spectroscopy of subcellular [Pi] on leaf 2016 samples from Temecula -collected xylem sap from Napa vineyard severely stunted 'sucker' rootstock 2016 samples; quantified P_i, sulfate, and nitrate by ion chromatography-flame ionization detection -methods development for anthocyanin quantitation by High Performance Liquid Chromatography-Mass Spectrometry/photodiode array detection	Tobacco vector transformations showed issue, but restriction-mapped vectors showed no re-arrangements; concluded the Agro strain suspect. RNA blot evidence for miR828 up-regulation by XF infection in CA samples. AtMYB75 and SPX DOMAIN (positive regulator of P_i starvation) strongly down-regulated by XF infection in Arabidopsis[5]. *TAS4c* and disease resistance leucine-rich-repeat receptors differential expression by XF provides evidence as causal effectors. Preliminary results of rootstock-derived XF-infected cane P_i show significant differences from control.
Dec. 2016 CDFA-PD Workshop	oral and poster presentations	Southern blot of Agrobacterium and *E. coli* CRISPR vectors show no host re-arrangements.
Mar. 2017 Interim Progress Report*	-completed degradome libraries 2015 CA samples -second attempt at grapevine rootstock 101-14 transformation initiated Feb. 2017 -qualify disease symptoms and quantify anthocyanins as significantly different in transgenic tobacco MYB90 repeat experiment -statistical analyses of differential expression of miRNAs and phasiRNAs in replicate transgenic MYB90 tobacco XF challenge experiments -statistical analyses of XF infection effects in 2015 CA samples by deep sequencing of small RNA and mRNA libraries confirms prior observation[6] in grapevine (eight weeks post-XF infection) for down regulation of target phosphate transporter *VvPHT2;1* and homologs, shown here inversely correlated with effector miR399 induction (which is phosphate-regulated). Similar results for phosphate-regulated miR827 and two *SPX* targets.	MAPMAN analysis of small RNA-Seq and mRNA-Seq CA 2015 libraries show inverse correlation between small RNAs and expression of template biotic stress genes, signaling receptor kinases (including candidate PdR1 locus *VIT_14s0171g00180*)[7], pathogenesis-related proteins and Pentatricopeptide repeat proteins, very strongly supporting the working model that XF infection results in compelling differential expression of mRNAs AND their derived phasiRNAs for ontology bins known to control pathogen resistance. RNA blot shows AtMYB90 overexpression in tobacco induces the endogenous negative siRNA regulator NtTAS4-3'D4(-) and its trigger miR828, supporting deep conservation of autoregulatory loop[8] and PD model. RNA blot analysis of transgenic tobacco corroborates statistical analysis of differential expression by deep sequencing that XF suppresses (down-regulates) MYB90→ TAS autoregulation activity and Nta-*MIR828ab* and *TAS4ab*, strongly

		supporting model. Successful production of transgenic tobacco harboring grapevine CRISPR vectors, demonstrating Agrobacterium host strain likely responsible for initial grapevine transformation problem. Repeat experiment of tobacco MYB90 challenge with XF successful.
July 2017 Year-end Progress Report*	-no cost extension granted until 12/31/17 -new PD field samples collected from Temecula (high quality fully expanded leaves and canes) and St. Helena CA -attempt to verify tobacco genome editing using grapevine synthetic guide vectors (long shot, due to low homology) -quantification of XF titres by qRT-PCR for repeat tobacco XF challenge experiment shows experiment successful, validating prior results. -further statistical analyses with DESeq2[9], ShortStack[10], and PhaseTank[11] of tobacco 2015 and 2016 libraries. Many novel miRNA candidates revealed -sleuth/kallisto[12] statistical analysis of 2015 CA mRNA-Seq libraries for stress- and auxin-inducible miR156, miR398, miR167, and miR393 grapevine targets reveal top leads for significantly down-regulated effectors of XF etiology upstream of miR828 and other P_i-regulated miR399 and miR827 -initiate replicate small RNA and degradome libraries from 2017 Temecula field PD samples and tobacco transgenic XF challenge experiments for more statistical power - quantify P_i, sulfate, and nitrate in 2017 stunted rootstock 'sucker' Napa PD samples and 2017 fully expanded PD Temecula scion samples by ion chromatography-flame ionization detection[13] -quantify by ^{31}P nuclear magnetic resonance the Aug. 2016 leaf PD samples. -quantify by mass spectrometry anthocyanins in 2017 Temecula xylem sap and leaves by visible wavelength spectroscopy. -visit Cooperator DLF lab to learn best practices re: XF microbiology. Initiate plate growth XF assays for phosphite	Grapevine somatic embryo regeneration proceeding well; some concern for MYBA6 transgenic regeneration. Principal Component Analysis of technical and biological replicate small RNA libraries made from 2015 and 2016 tobacco XF challenge experiments demonstrated that biological variables of genotype and condition were reproducible. Statistically significant mis-regulated miRNAs in replicate XF challenged transgenic tobacco libraries further documented; Nta-miR399, miR828, and *TAS4ab* changes correlate (down in XF) with prior RNA blot and preliminary statistical results, showing *MIR828/TAS4* autoregulatory loop effects. Nta-miR827 and miR156 up-regulated, consistent with working model where SPL targets of miR156 down regulate anthocyanin biosynthesis in Arabidopsis[14], providing a direct link/mechanism for how VvMYBA6/7 and other miR828 MYB targets in grapevine are deranged by XF infection resulting in anthocyanin accumulation. Results of P_i quantitation by two methods of fully expanded leaves and canes in 2016 and 2017 Temecula PD samples support hypothesis that XF infection results in significantly lower [P_i] (about 60% decrease) in host leaf and xylem sap. Correlates with elevated anthocyanins quantified in PD xylem sap by mass spectrometry and leaves by spectrophotometry. Further substantiated by prior results for other grape cultivars[15, 16], supporting working model.
Dec. 2017 CDFA-PD Proceedings^	- regeneration of grapevine transformants - 18 degradome, 8 sRNA, and 12 stranded mRNA transcriptome 2017 field sample libraries in preparation, including 'green island' cane bark and 'matchstick petiole' samples - leaf anthocyanin quantitation by uHPLC spectrophotometry - plate growth quantitative assay developed for	Transgenics on track for completion Dec. 2017 Quantitation of anthocyanins cyanin and malvin and aglycone species in leaf samples by uHPLC-spectrophotometry LD_{50} ~ 5mM determined for phosphite

	phosphite inhibition of XF	inhibition of XF in plate growth assay
This report	- regeneration of grapevine transformants nearly complete - quantify XF titers in concordant petioles, qPCR - re-quantify hydrolyzed anthocyanins in leaves and extend to xylem sap by uHPLC spectrophotometry - LD_{50} repeat experiment for phosphite inhibition of XF plate growth - XF challenge of tobacco plants safened with phosphite pre-treatments - manuscript preparation	Cooperator confirmed shipment of potted plants within few weeks. Degradome and sRNA field sample libraries shipped to UC-R IIGB and sequenced; data in IIGB bioinformatics queue for demultiplexing and release to PI. Validate prior results: anthocyanins higher in XF leaves and xylem sap. Validate LD_{50} < 3 mM for phosphite. XF challenge experiments with Phi ongoing.
^ available at https://www.cdfa.ca.gov/pdcp/Research.html *available at http://www.piercesdisease.org/reports		

OBJECTIVES (as originally funded; Objective III was added at the amended award stage in 2016, and Objective I rephrased in 2016 [shown in *italics*])

I. Test the miR828, *TAS4*, and target *MYBA6/7* functions in PD etiology and XF infection and spreading by genome editing using CRISPR/Ca9 transgenic technology. Rephrased in 2016: *Demonstrate the efficacy of CRISPR/Cas9 transgenic technology for creating deletion mutants in* MIR828, TAS4*, and target* MYBA6/7. *When validated, future experiments will critically test these genes' functions in PD etiology and XF infection and spreading.*

II. Characterize tissue-specific expression patterns of *TAS4* and *MIR828* primary transcripts, small RNAs, and *MYB* targets in response to XF infections in the field, and in the greenhouse for tobacco transgenic plants overexpressing *TAS4* target gene *AtMYB90/PRODUCTION OF ANTHOCYANIN PIGMENT2*.

III. Characterize the changes in (a) xylem sap and leaf P_i, and (b) polyphenolic levels of XF-infected canes and leaves. (c) Test on tobacco in the greenhouse and XF growth *in vitro* the P_i analogue phosphite as a durable, affordable and environmentally sound protectant/safener for PD.

RESULTS AND DISCUSSION

I. Test the miR828, *TAS4*, and target MYBA6/7 functions in PD etiology and XF infection and spreading by genome editing using CRISPR/Cas9 transgenic technology

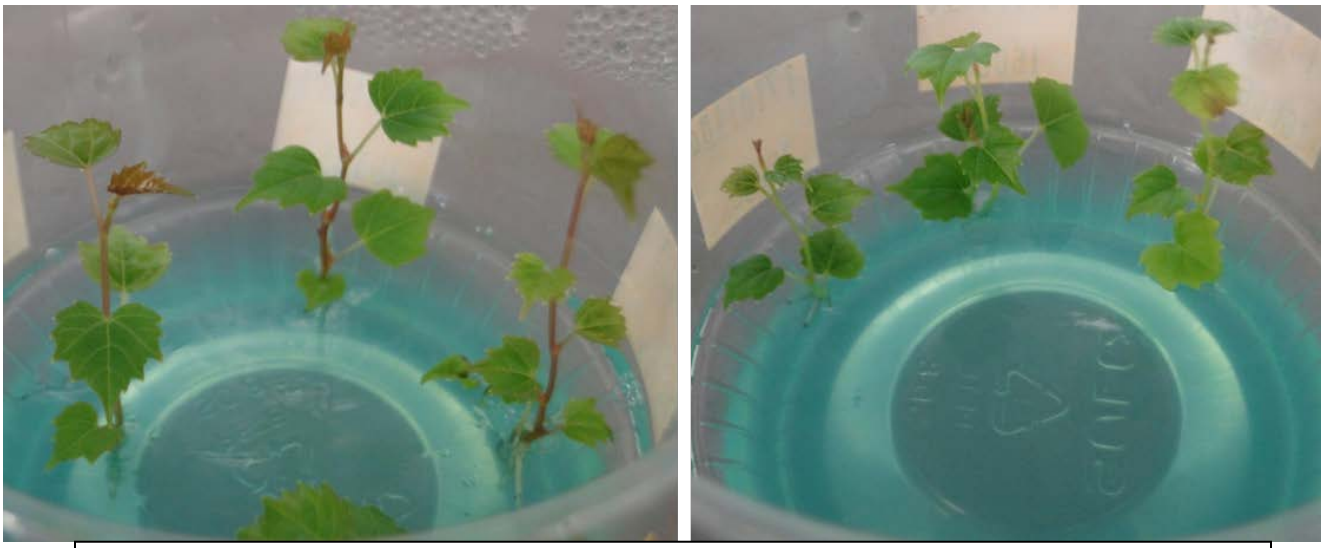

Fig. 1. Progress of regeneration of grapevine transformants of p201-N-Cas9 vector constructs harbored in Cooperator-sourced EHA105 *Agrobacterium* strain, initiated Feb. 2017. **Left:** MYBA6. **Right:** MYBA7. MIR828, TAS4a, TAS4b, control empty vector: not shown.

Ongoing regeneration of plantlets from somatic embryos produced from rootstock 101-14 grape transformations with five CRISPR binary T-DNA vectors (plus empty vector control) in the lab of Cooperator DT were reported in the July 2017 and October 2017 Interim Progress Reports. **Figure 1** shows the current status of representative materials for the MYB effector constructs. Dr. Tricoli claims he will deliver potted plants (under duly issued APHIS-BRS permit # 17-342-101m) and complete the fee-for-service contract initiated in Nov. 2015 within a few weeks. Validation of editing events going forward will be by PCR cloning and sequencing of target genes, and polyacrylamide gel electrophoresis-based genotyping[17].

II. Characterize tissue-specific expression patterns of *TAS4* and *MIR828* primary transcripts, siRNAs, and *MYB* targets in response to XF infections in the field.

We sent in Dec. 2017 to the Institute of Integrative Genome Biology, UC Riverside a complete set of Illumina libraries with biological replicates for small RNAs, stranded mRNAs, and degradome samples from the 2017 Calle Contento Temecula field leaf samples, and the 2016 replicated greenhouse XF tobacco MYB90 overexpression experiment. In addition we prepared indexed libraries for 'green island' cane bark and 'matchstick petiole' samples from the 2017 Temecula field expedition for discovery of differential miRNA expressions associated with diagnostic, yet pleiotropic, PD traits hypothesized to be due to deranged small RNA activities. Two runs of HighSeq500 (400m reads per run) have been completed in Dec. 2017 and the data await demultiplexing and release. The delay was due to the Holiday break when the campus was closed, and in the new year due to staff on maternity leave and sick leave. There are eight small RNA libraries to pooled and indexed with 18 degradome samples, and 12 stranded mRNA-Seq transcriptome libraries sequenced separately. This level of complexity will result in ~12 million reads per small RNA library, and ~25 million reads per transcriptome library. All workflow processes and yields were verified as optimal/appropriate through the data analysis and genome annotation stages. The statistical power from multiple replicates across years will allow defensible claims at the publication stage, which in in process and will be completed when the sequencing data is made available in the next few weeks.

III. Characterize the changes in (a) xylem sap and leaf Pi, and (b) polyphenolic levels of XF-infected canes and leaves. (c) Test the P_i analogue phosphite on tobacco in the greenhouse and XF growth *in vitro* as a durable, affordable and environmentally sound protectant/safener for PD.

(a) Xylem sap [Pi]. In May 2017 the PI collected PD samples from Malbec rootstock sucker canes from Napa Co Phelps vineyard (1109 Silverado Trail South, River Ranch Farm Workers Housing, St. Helena CA) and healthy control scion canes under the supervision of UC eXtension agent Dr. Monica Cooper, and Merlot variety PD and control samples in June 2017 from the Calle Contento vineyard in Temecula CA. The Merlot variety leaves and canes from Temecula PD symptomatic scion samples were not developmentally stunted, allowing appropriate side-by-side controlled genotype and developmental state comparisons. We reported in the July 2017 Interim Progress Report the results from both ^{31}P nuclear magnetic resonance from 2016 Temecula leaf samples and ion chromatography of 2017 Temecula xylem sap samples that support the working hypothesis that PD-infected canes and leaves have significantly lower P_i (~60%) concentrations than healthy controls. We plan to collect more material in 2018 to further substantiate and verify our results.

(b) Polyphenolics in XF-infected canes and leaves. We reported in the July 2017 Interim Progress Report results for mass spectrometric quantification of cyanin and malvin in xylem sap from the Temecula June 2017 field samples, and anthocyanins in leaves. We are in the process of quantifying XF titers in concordant petioles samples from these leaf and cane samples by real time-PCR. The results directly support the hypothesis that XF infection results in accumulation of anthocyanins in xylem sap and leaves. Similar results have been reported for procyanidins and other polyphenolics in xylem sap two months post-XF infection in Thompson

seedless and several winegrape cultivars[15, 16]. Phenolic levels in Merlot xylem sap correlate with PD severity compared to other cultivars[18].

In an effort to characterize the anthocyanin complexity in 2017 Temecula leaf samples, we developed quantitative high performance liquid chromatography-spectrophotometic methods for malvin (a di-O-methylated anthocyanidin [less polar]) and cyanin, and their hydrophobic aglycones malvidin and cyanidin generated after acid + heat hydrolysis. We employ an Acclaim Pepmap RSLC 75 µm x 15 cm nanoViper C_{18} 2 µm reverse phase column coupled to a photodiode array detector (530 nm)[19] with 95% water:formic acid as stationary phase and 100% acetonitrile as mobile phase, linear gradient from 5-100% mobile in 40'. **Fig. 2A** shows a standard curve derived for cyanin, and chromatogram traces of unhydrolyzed (**Fig. 2B**) and mono-/di-aglycone (hydrolyzed, **Fig. 2C**) PD leaf samples. There are other abundant peaks eluting at later times (18.07'), which are likely other anthocyanins but some peaks (e.g. ~19.1') are concordant with single- and/or double-aglycones of cyanin and malvin, based on hydrolysis timecourse experiments with standards (data not shown).

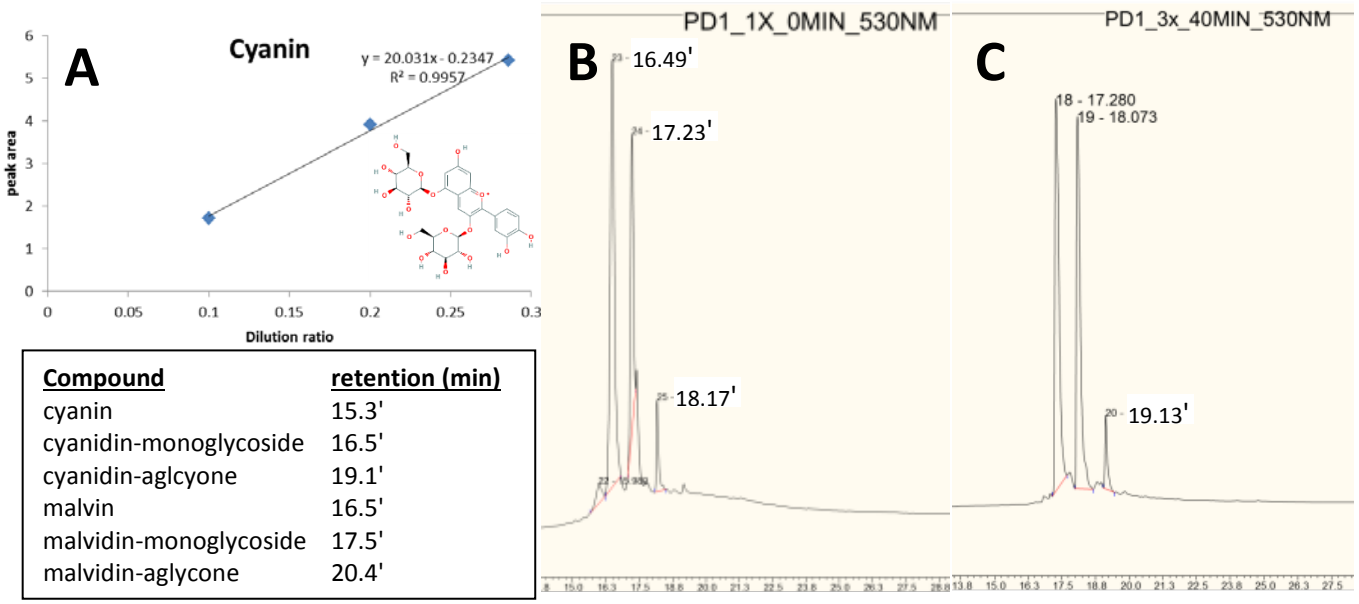

Compound	retention (min)
cyanin	15.3'
cyanidin-monoglycoside	16.5'
cyanidin-aglcyone	19.1'
malvin	16.5'
malvidin-monoglycoside	17.5'
malvidin-aglycone	20.4'

Fig. 2. High performance reverse phase liquid chromatography for quantitation of anthocyanins cyanin and malvin and aglycone species in leaf samples. **A)** Standard curve for cyanin. Structure inset. **B)** Chromatogram of unhydrolyzed Temecula 2017 PD leaf sample extract, showing major peaks of malvin and/or cyanidin-monoglycoside (retention times ~16.5'), possibly malvidin-monoglycoside (~17.23') and uncharacterized anthocyanin (18.17'). **C)** Chromatogram of acid hydrolyzed PD extract supports cyanin identification (peak 22 in panel B) by detecting aglycone species (19.13'), and peak 19 possibly as monoglycoside (see panel B, peak 25).

Fig. 3 below shows new results for semi-quantitative analysis of cyanin-monoglycoside in XF-infected xylem sap by uHPLC-photodiode array spectrophotometry. Although the limited amounts of material available after phosphate quantitations precluded absolute quantitation, there was clearly a marked increase in cyanidin in XF-infected xylem sap. Taken together these results support our working hypothesis that the xylem sap anthocyanins and other polyphenolics are important for PD disease progression.

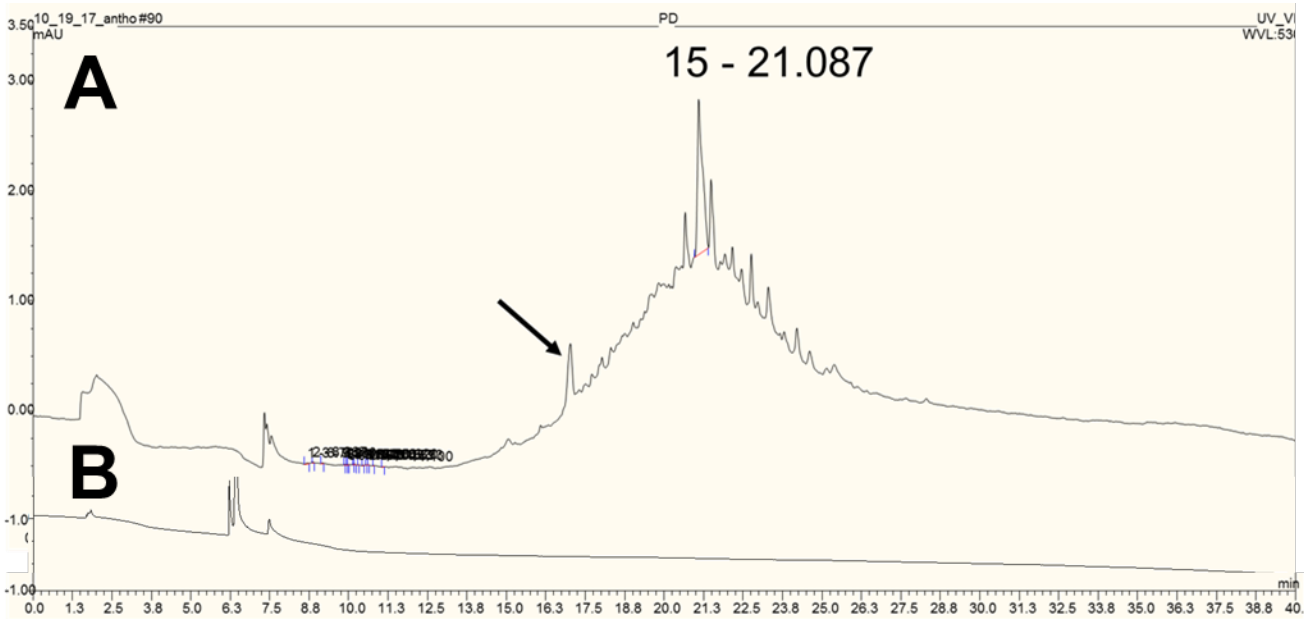

Fig. 3. Ultra high performance reverse phase liquid chromatography for quantitation of cyanidin-monoglycoside (retention time ~16.5'; arrow) in **A)** xylem sap sample from XF-infected canes. **B)** No peaks were detected with control

(c) P_i analogue phosphite as effector of XF growth and safener of disease symptoms.

Figure 4 reports results of a baseline study for XF growth on PD2 potato starch plates[20] (P_i component omitted and 2 g/L potato starch substituted for bovine serum albumin) as a function of physiological

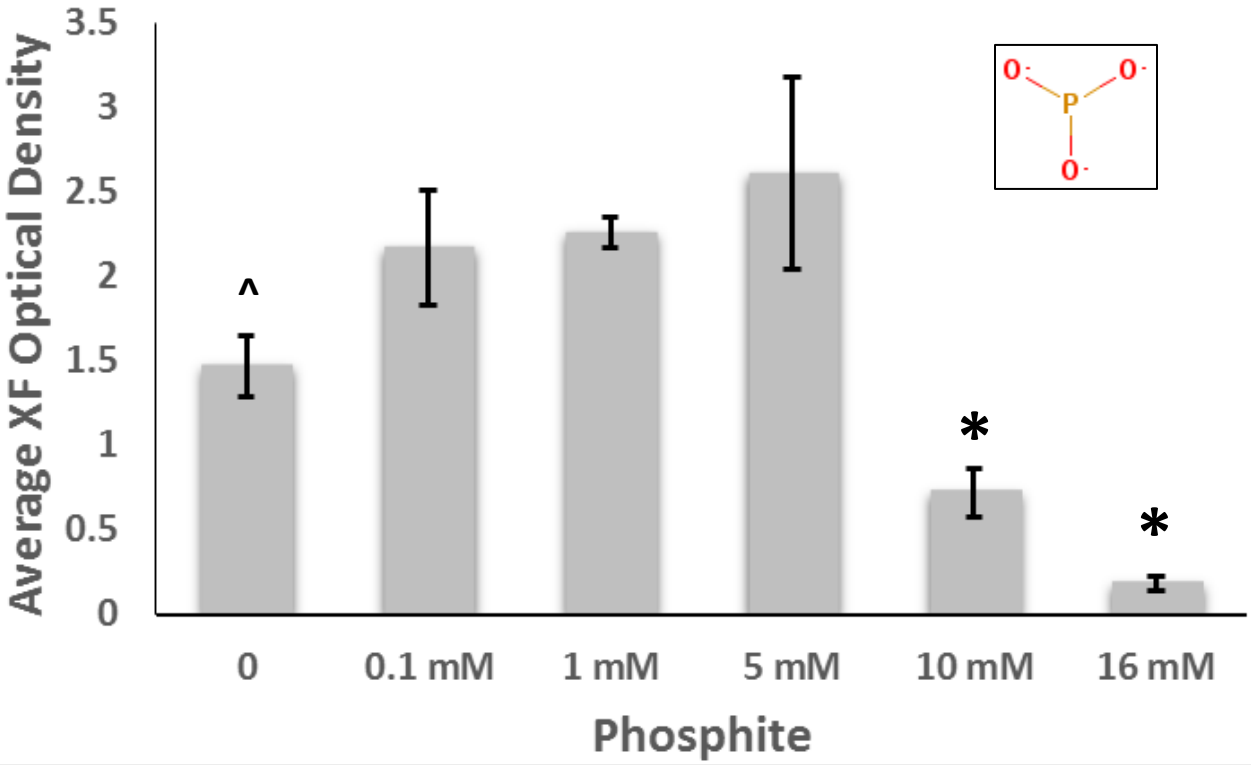

Fig. 4. Physiological concentrations of phosphite (structure inset) inhibit plate growth of XF. Asterisk (*) indicates significantly different than 0- 5 mM treatments, $P < 0.004$ (Student's two-sided t test, equal variance assumed). ^: not significantly different than 0.1- 5 mM treatments. Error bars are s.e.m. (n =3, except 0 and 0.1 mM treatments, n =2).

concentrations of phosphite added to XF minimal growth medium. This experiment has been repeated twice at lower growth densities and including standard medium P_i concentration (16 mM) to facilitate more quantitative and physiologically relevant results normalized to colony-forming units.

Figure 5 reports new results of a repeat experiment similar to reported in the Oct. 2017 Proceedings report which provides conclusive evidence that phosphite can function as an active competitor of physiological concentrations of P_i influencing XF plate growth, with a LD_{50} < 3 mM. (application concentration for lethal dose). Ongoing work is focused on testing phosphite as safener for tobacco plants challenged with XF in the greenhouse.

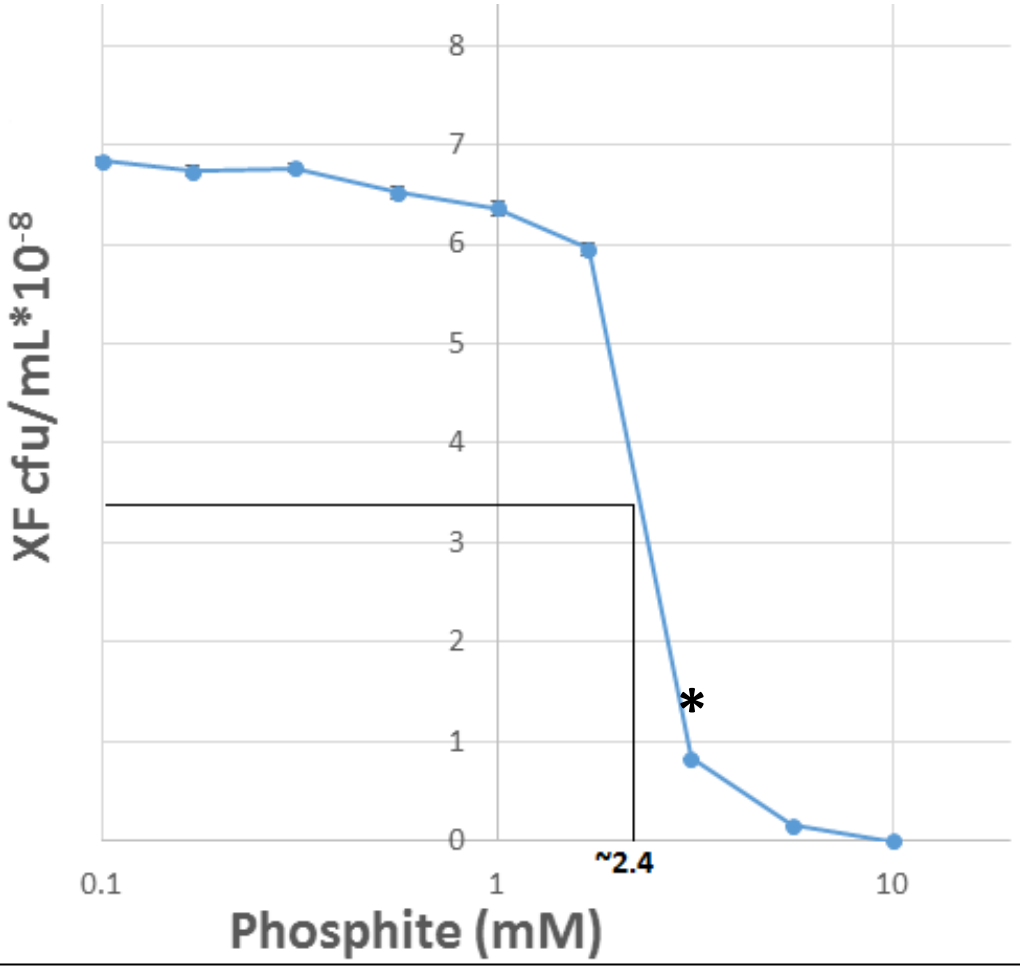

Fig. 5. Phosphite has an LD_{50} of < 3 mM for plate growth of XF. Error bars are s.e.m. (n =7-9). Asterisk (*) indicates significantly different than zero phosphite control, $P < 10^{-6}$ (Student's two-sided t-test, equal variance assumed).

CONCLUSIONS

We have achieved our Objectives within the time frame of two years' funding (plus six month no cost extension). We have generated compelling evidence supporting our working model for *MIR828/TAS4* genes, identified new lead target genes, and presented evidence that phosphite impacts XF growth. This latter result underscores the practical value of the project to develop a durable management tool while generating new knowledge about PD etiology and engineered resistance.

REFERENCES CITED

1. Jacobs T, LaFayette P, Schmitz R, Parrott W (2015) **Targeted genome modifications in soybean with CRISPR/Cas9**. *BMC Biotechnol* **15**: 16
2. Mali P, Yang L, Esvelt KM, Aach J, Guell M, DiCarlo JE, Norville JE, Church GM. (2013) **RNA-guided human genome engineering via Cas9**. *Science* **339**: 823-826
3. De La Fuente L, Parker JK, Oliver JE, Granger S, Brannen PM, van Santen E, Cobine PA (2013) **The bacterial pathogen *Xylella fastidiosa* affects the leaf ionome of plant hosts during infection**. *PLoS ONE* **8**: e62945
4. Velten J, Cakir C, Youn E, Chen J, Cazzonelli CI (2012) **Transgene silencing and transgene-derived siRNA production in tobacco plants homozygous for an introduced *AtMYB90* construct**. *PLoS ONE* **7**: e30141
5. Rogers EE (2012) **Evaluation of *Arabidopsis thaliana* as a model host for *Xylella fastidiosa***. *Mol Plant-Microbe Interact* **25**: 747-754
6. Choi H-K, Iandolino A, da Silva FG, Cook DR (2013) **Water deficit modulates the response of *Vitis vinifera* to the Pierce's disease pathogen *Xylella fastidiosa***. *Mol Plant-Microbe Interact* **26**: 643-657
7. Walker MA, Agüero CB, Riaz S, Dandekar AM: **Molecular and functional characterization of the putative *Xylella fastidiosa* resistance gene(s) from b43-17 (*Vitis arizonica*)**. In: *Pierce's Disease Research Progress Reports.* Edited by Esser T. Sacramento, CA: California Department of Food and Agriculture; 2013: 208-213.
8. Luo Q-J, Mittal A, Jia F, Rock CD (2012) **An autoregulatory feedback loop involving *PAP1* and *TAS4* in response to sugars in Arabidopsis**. *Plant Mol Biol* **80**: 117-129
9. Love MI, Huber W, Anders S (2014) **Moderated estimation of fold change and dispersion for RNA-seq data with DESeq2**. *Genome Biol* **15**: 550
10. Johnson NR, Yeoh JM, Coruh C, Axtell MJ (2016) **Improved placement of multi-mapping small RNAs**. *G3: Genes|Genomes|Genetics* **6**: 2103-2111
11. Guo QL, Qu XF, Jin WB (2015) **PhaseTank: genome-wide computational identification of phasiRNAs and their regulatory cascades**. *Bioinformatics* **31**: 284-286
12. Pimentel HJ, Bray N, Puente S, Melsted P, Pachter L (2017) **Differential analysis of RNA-Seq incorporating quantification uncertainty**. *Nat Meth* **14**: 687-690
13. Jackson LK, Joyce RJ, Laikhtman M, Jackson PE (1998) **Determination of trace level bromate in drinking water by direct injection ion chromatography**. *J Chromatog A* **829**: 187-192
14. Gou J-Y, Felippes FF, Liu C-J, Weigel D, Wang J-W (2011) **Negative regulation of anthocyanin biosynthesis in Arabidopsis by a miR156-targeted SPL transcription factor**. *Plant Cell* **23**: 1512-1522
15. Wallis CM, Chen J (2012) **Grapevine phenolic compounds in xylem sap and tissues are significantly altered during infection by *Xylella fastidiosa***. *Phytopathology* **102**: 816-826
16. Wallis CM, Wallingford AK, Chen J (2013) **Grapevine rootstock effects on scion sap phenolic levels, resistance to *Xylella fastidiosa* infection, and progression of Pierce's disease**. *Front Plant Sci* **4**: 502
17. Zhu X, Xu Y, Yu S, Lu L, Ding M, Cheng J, Song G, Gao X, Yao L, Fan D, Meng S, Zhang X, Hu S, Tian Y (2014) **An efficient genotyping method for genome-modified animals and human cells generated with CRISPR/Cas9 system**. *Sci Rep* **4**: 6420
18. Wallis CM, Wallingford AK, Chen J (2013) **Effects of cultivar, phenology, and *Xylella fastidiosa* infection on grapevine xylem sap and tissue phenolic content**. *Physiol Mol Plant Pathol* **84**: 28-35
19. Zhang Z, Kou X, Fugal K, McLaughlin J (2004) **Comparison of HPLC methods for determination of anthocyanins and anthocyanidins in bilberry extracts**. *J Agric Food Chem* **52**: 688-691
20. Davis MJ, Purcell AH, Thomson SV (1980) **Isolation media for the Pierce's disease bacterium**. *Phytopathology* **70**: 425-429

FUNDING AGENCIES

Funding for this project was provided by the CDFA Pierce's Disease and Glassy-winged Sharpshooter Board, Agreement Number 15-0214-SA.

ACKNOWLEDGEMENTS

The authors thank Carmen Gispert, Greg Pennyroyal, and Monica Cooper for access to Temecula and St. Helena CA vineyards; Glenn Hicks for bench space and Illumina Nextseq500 sequencing at the UCR Institute for Integrative Genome Biology; the Texas Tech Center for Biotechnology and Genomics for assistance with HPLC and mass spectrometry; and the TTU High Performance Computer Center for support in use of the Quanah supercluster.